

Grave-to-cradle dry reforming of plastics via Joule heating

Received: 1 April 2024

Accepted: 10 September 2024

Published online: 20 September 2024

Check for updates

Qing Ma¹, Yongjun Gao¹✉, Bo Sun², Jianlong Du¹, Hong Zhang¹ & Ding Ma²✉

Both plastics and CO₂ are waste carbon resources, and their accumulation in nature has led to severe environmental pollution. However, simultaneously converting plastic waste and CO₂ into value-added chemicals remains a challenge. Here we demonstrate a catalytic reforming process that converts plastics and CO₂ into syngas over an electrified FeCrAl heating wire. The temperature of the electrified heating wire can quickly exceed 800 °C, facilitating the decomposition of polyethylene into gaseous hydrocarbons. The high-temperature heating wire promote the CO₂ deoxygenation, resulting in the generation of CO, as well as the dehydrogenation of gaseous hydrocarbons. Significantly, the additional O species from CO₂ and the carbon species from hydrocarbons can react to form CO, maintaining the high catalytic activity of the electrified heating wire. This novel approach is of paramount to achieving a circular economy in addressing the ongoing environmental crisis caused by the accumulation of plastic waste and excessive CO₂ emissions.

Statistically, over 380 million tons of plastics are produced annually worldwide^{1–4}. However, the majority of these plastics enter the environment after a short service life and cannot naturally degrade, leading to critical environmental pollution and ecological crises. Only a small proportion of plastic waste was recycled to produce low-quality plastic products or burned to recover chemical energy. Although incineration is an efficient strategy to dispose of solid plastic waste and generate heat for power generation, huge CO₂ emissions are unavoidable. In addition, due to the incomplete combustion or presence of the nitrogen or sulfur-containing additives in plastics, some gaseous pollutants such as polycyclic aromatic hydrocarbons, NO_x and SO_x are generated⁵. From an environmental protection perspective, there is an urgent need to develop a green and sustainable strategy to dispose of plastic waste accumulated in the environment. Moreover, with the rapid development of the society and the rapid improvement of the level of industrialization, approximately 36.5 Gigatons of CO₂ are generated each year⁶. The increasing concentration of CO₂ in the atmosphere contributes to the greenhouse effect, resulting in severe global warming and posing a threat to the survival of all living

organisms. Therefore, it is crucial to develop technologies or strategies to address these environmental challenges.

Plastic waste and CO₂ can be considered valuable carbon resources because they can potentially be converted into fuels and valuable chemicals. Through various catalytic processes such as high-temperature pyrolysis, catalytic pyrolysis, or catalytic hydrogenolysis, waste plastics can be depolymerized and transformed into fuels or other valuable chemicals^{7–11}. CO₂ can also be hydrogenated to carbon monoxide, methane, methanol or other hydrocarbon over transition metal catalysts^{12–14}. In addition, the reaction between CO₂ and methane at high temperatures over reforming catalysts can produce syngas^{15–18}. Building on this reaction, it is possible to explore the idea of using waste plastics such as polyethylene and polypropylene as a replacement for methane in the reforming process with CO₂ to produce syngas^{19–21}. However, the unique structure of polyolefins, which consists of inert C-C bonds in the backbone^{22,23}, poses a challenge in efficient CO₂ reforming of plastics compared to traditional methane reforming. Furthermore, the selectivity towards syngas is often compromised due to the presence of methane, hydrocarbons, and coke^{24,25}.

¹Hebei Research Center of the Basic Discipline of Synthetic Chemistry, College of Chemistry and Materials Science, Hebei University, Baoding, China. ²Beijing National Laboratory for Molecular Sciences, New Cornerstone Science Laboratory, College of Chemistry and Molecular Engineering, Peking University, Beijing, China. ✉e-mail: yjgao@hbu.edu.cn; dma@pku.edu.cn

Therefore, it becomes crucial to employ higher reaction temperatures and excellent catalysts to improve conversion efficiency^{15,19}.

The traditional approach of burning fuel to provide heat at higher temperatures leads to undesirable CO₂ emissions. Along with the increase of availability and accessibility of green and sustainable electricity from sun and wind, using electricity energy to heat chemical reactor is a promising way to achieve the decarbonization of chemical process. The microwave heating, induction heating and Joule heating are the three ways to achieve the electricity-to-heat process, which have their special advantages and limitation due to the different power-to-heat principles²⁶. Among the three electricity-to-heat ways, the Joule heating has a theoretical energy efficiency of 100% because it directly transforms electricity to heat by driving charge carriers to flow through conductor to generate high temperature²⁷. By electrifying the catalyst, or support for active phase, or reactor wall, the higher reaction temperature required for reactions can be achieved instantly, avoiding heat transfer as in the conventional heating process and the transformation of electrical energy into electromagnetic energy as in microwave heating and induction heating. The fast heating rate and uniform heat distribution contribute to higher reaction efficiency, which translates into lower CO₂ emission. Recently, the application of electrified spatiotemporal heating techniques has shown the potential to depolymerize polyolefins into their respective monomers with relatively high yields²⁸. Additionally, the flash Joule heating process has been successful in converting waste plastics into flash graphene along with byproducts such as hydrogen and light hydrocarbons^{28–30}. It is evident that the degradation or transformation of plastics through rapid electric heating technology follows a distinct mechanism. Therefore, developing a new catalytic approach for CO₂ reforming of waste plastics with high efficiency, low energy consumption, zero carbon emissions, or even sustainable properties is of great importance. In this report, we develop a novel and sustainable catalytic system for the efficient and selective conversion of waste plastic and CO₂ into syngas. In order to ensure an environmentally friendly and sustainable process, a photovoltaic power system was used to supply energy. Consequently, the reforming of plastics with CO₂ to syngas can be carried out under sunlight irradiation.

The green and sustainable electricity generated is passed through an iron-chromium-aluminum (FeCrAl) heating wire, generating high temperature via Joule heating, which promotes the decomposition of polyolefins into gaseous hydrocarbons through melting, gasification and fission. Subsequently, the small-molecule hydrocarbons and CO₂ undergo reforming, resulting in the formation of CO and H₂ on the surface of the electrified FeCrAl heating wire. In laboratory tests, we successfully reformed 14 mg of polyethylene (approximately 1 mmol of carbon) and 1 mmol of CO₂ into CO and H₂ in just 15 min, which can be scaled up to large scale reforming of 1 g of PE and 3.3 g of CO₂. Combined with the mature post-combustion CO₂ capture technology, such as cyclic adsorption/desorption by using amine-based solvents, up to 90% of CO₂ emission from industrial processes and power generation will be captured and used for reforming with plastic to produce syngas³¹. Moreover, the FeCrAl heating wire used in this system possesses excellent coke resistance property, and the electrons flowing through the heating wire promote the reforming reactions. This innovative catalytic system presents an efficient approach to transform two wastes, plastics and CO₂, into value-added chemicals simultaneously.

Results

Plastics reforming with CO₂

FeCrAl alloy is a resistance heating material that exhibits exceptional oxidation resistance at high temperatures³². This outstanding property has led to its widespread use in various heating devices. In addition, FeCrAl alloy exhibits high resistance to coke formation, making it a

suitable catalyst support for numerous industrial applications^{32,33}, including automotive exhaust treatment^{32,34}, CH₄ oxidation^{32,35}, and Fischer–Tropsch synthesis^{32,36,37}. In our study, a reactor being composed of one quartz tube (outer diameter: 25 mm, inner diameter: 19 mm, length 100 mm), a length of spring-like FeCrAl heating wire (diameter: 0.3 mm), a porcelain boat as sample holder, a pair of metal flange seals equipped with two ball valves and two copper wires was designed so that the heating wire can be electrified and used as key component to promote the reaction involving plastics and CO₂ in a sealed environment. The actual temperature around the heating wire in the reactor can be measured by a thermocouple installed in the reactor (Fig. 1a and Supplementary Fig. 1). During our research, a piece of heating wire with a resistance value of 6 ohms was electrified by a direct current (DC) power generator (MAISHENG, MP3030D) in the reactor containing 14 mg of polyethylene (PE) powder and being full of argon gas. The gas products can be quantified by a gas chromatograph and the residual carbon can be determined by weighing the total mass of main parts of the reactor before and after reaction, including the quartz tube, porcelain boat and resistance wire (Supplementary Table 1). Under the conditions of 4 amperes current for 15 minutes, 0.998 mmol H₂ was achieved according to the quantify result of gas chromatograph except of the negligible hydrocarbons, CO and CO₂ (Supplementary Table 2). The trace amount of oxygen and positive deviation of mass or carbon balance may come from the FeCrAl heating wire because there are 2.06 wt% oxygen and 6.57 wt% carbon according to energy dispersive X-ray microanalysis of scanning electron microscope (SEM-EDS, Supplementary Fig. 2). The mass of the residual carbon was about 12 mg, indicating the successful dehydrogenation of PE (Fig. 1b). To maximize the utilization of the carbon deposition derived from PE, CO₂ was introduced into the system, with the expectation that it would react with PE to produce syngas and with coke to produce CO. As depicted in Fig. 1b, with the increase in the initial concentration of CO₂, the amount of CO produced increased, while the mass of carbon deposition decreased. When 1 mmol of CO₂ was introduced into the system, approximately 0.71 mmol of H₂, 1.70 mmol of CO, and trace amounts of light hydrocarbons (CH₄, C₂H₄, etc.) were produced. The conversion of CO₂ reached 88% with complete conversion of PE. The decrease in the amount of H₂ compared to the dehydrogenation of pure PE can be attributed to the hydrogenation of a small amount of CO₂. To eliminate carbon deposition entirely, the amount of CO₂ in the reactor was increased to 1.25 equivalents of carbon in PE, resulting in a slight decrease in the amount of H₂, no significant change in the amount of CO, and a slight increase in the amount of remaining CO₂ in the system. Thus, conditions involving 1 mmol of PE and 1 mmol of CO₂ as starting reactants were selected for subsequent research.

As shown in Fig. 1c, the resistance and current of FeCrAl heating wire were further screened based on the optimized conditions. At current value of 4 amperes, the 4 ohms heating wire provided lower amounts of H₂ and CO, while the yields of solid carbon and methane increased. Decreasing the resistance value to 2 ohms, the negligible H₂ and a tiny amount of CO can be detected, with a large proportion of CO₂ and PE remaining. If the resistance value was 1 ohm, the CO₂ reforming of PE cannot occur. Moreover, it was observed that the temperature in the reaction system decreased along with the decrease in the resistance value of the heating wire. This decrease in temperature can be explained by Joule's heating law $Q = I^2Rt$. On the other hand, when keeping the resistance value constant at 6 ohms and decreasing the current value during the reaction, the yield of H₂ and CO decreased obviously. Furthermore, the reforming reaction did not occur at 2 or 1 ampere, although the reaction temperature reached 150–350 °C. It is important to note that other resistance and current values were also tested and the results were not ideal. These results highlight the importance of reaction temperature in promoting CO₂ reforming of PE.

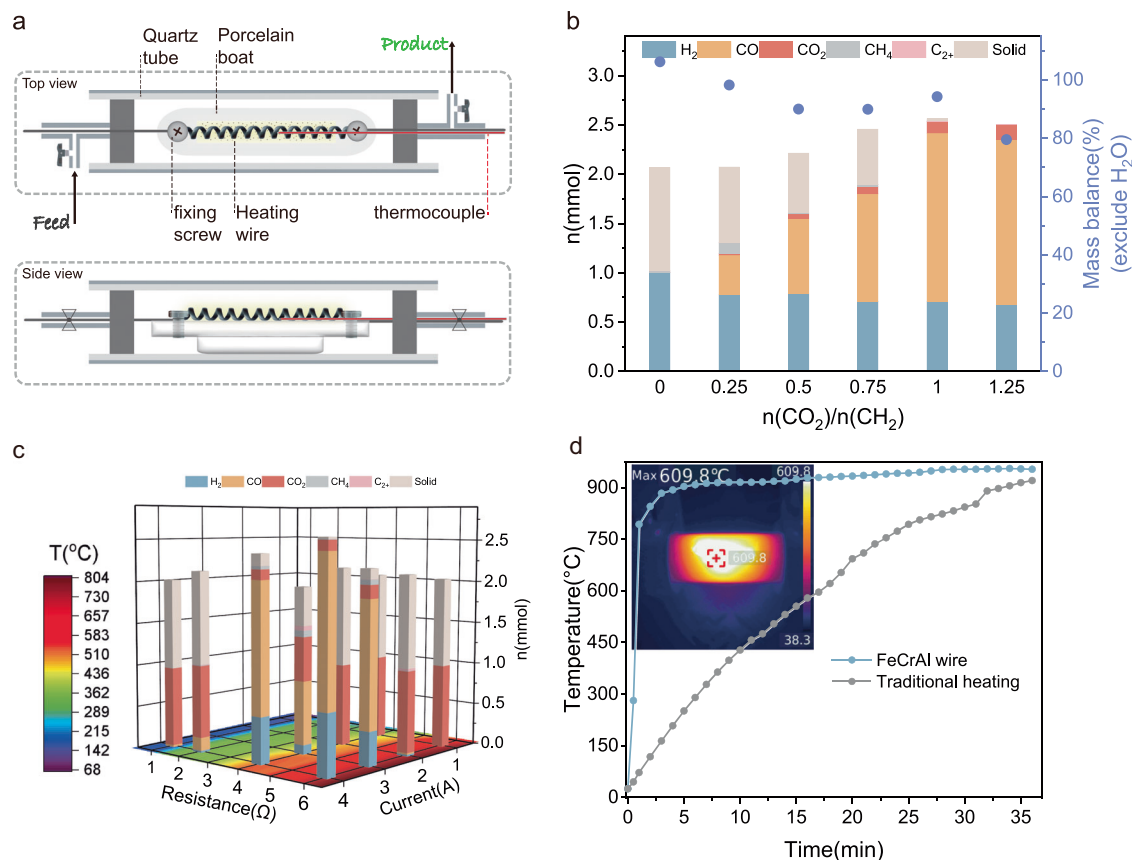


Fig. 1 | Reactor configuration and reaction conditions screening. **a** Schematic of an electrified reactor for CO₂ reforming of plastics; **b** products distribution with different mole ratio of CO₂ to CH₂ in PE (n(CO₂)/n(CH₂)). Reaction conditions: PE = 14 mg, FeCrAl heating wire 6 Ω, current 4 A, T = 800 °C, 15 min; **c** the product distribution over temperature profile under different current and resistance values;

Reaction conditions: PE = 14 mg, n(CO₂)/n(CH₂) = 1, FeCrAl heating wire, 15 min. the temperatures were measured by a thermocouple; **d** the heating rates of electrified FeCrAl heating wire (power = 96 W) and traditional tube furnace (power = 1000 W), the temperatures for the profiles were measured by a thermocouple, the inserted thermal image was recorded by a thermal camera (UTi-260B).

One of the advantages of using FeCrAl heating wire (power is 96 W) as a heating element and catalyst in the catalytic system is the fast heating speed. In contrast to the traditional heating strategy with a tube furnace over 30 minutes, by using FeCrAl heating wire, the radiation temperature near PE in the reactor can reach up to 800 °C within 30 s (Fig. 1d), melting solid PE into liquid, which indicates an energy-saving catalytic system. The commercially available FeCrAl heating wire consists of approximately 70 wt% Fe, 25 wt% Cr, and 5 wt% Al³⁸. We assume that the heating wire itself acts as a catalyst, promoting the reactions. To test this hypothesis, various heating units were evaluated as substitutes for the FeCrAl heating wire to promote CO₂ reforming of PE (Fig. 2a). All experiments in Fig. 2a were performed at the same temperature of 650 °C. First, the NiCr heating wire, which can provide reaction temperature of 650 °C, was evaluated under identical conditions. While the amount of H₂ produced in the system was slightly lower than that of the FeCrAl heating wire, with a decreased yield of CO and an increased generation of carbon deposition. The coke can be clearly observed on the surface of the NiCr heating wire after the reaction because the nickel element has the property of carbon permeation. Using a carbon fiber as a heating element, CO₂ reforming of PE was also observed, with a slightly higher H₂ yield of 57.3% and a lower CO yield of 59.1%, but more residual solid of 14.5%. (the detailed products distribution of carbon fiber and SEM images are showed in Supplementary Table 3 and Supplementary Fig. 3). However, only 0.6% of solid was left with FeCrAl heating wire as heating component at 650 °C, demonstrating that the FeCrAl heating wire is an efficient catalyst for promoting the reforming reaction, but not the key factor. To further confirm this point, a long length of FeCrAl heating

wire was wrapped around the quartz tube to allow rapid heating from the outside. The reaction temperature was monitored using an instrument connected to a thermocouple positioned in the quartz tube. Although the temperature in the quartz tube quickly reached about 650 °C and remained constant for 15 min, the reforming reaction did not occur, and PE only decomposed into light hydrocarbons (outside). Similarly, when a length of FeCrAl heating wire was placed in the system but not powered, and the temperature was provided by a wrapped heating wire outside the quartz tube (out-inside), only a negligible amount of CO and H₂ could be detected. Furthermore, the CO₂ reforming of PE was inhibited when the FeCrAl heating wire was embedded in Al₂O₃ porcelain, even though the porcelain was electrified and reached a temperature of 650 °C in the quartz tube. These results collectively suggest that only the electrified FeCrAl heating wire, capable of reaching high temperatures, can effectively promote the CO₂ reforming of PE. In other words, it is an electro-assisted catalytic process. The hot electrons flowing through the heating wire likely play an essential role in activating PE and CO₂, as previously mentioned in studies highlighting the catalytic properties of electrons^{39,40}.

Under the optimized conditions, this electrified catalytic system can also catalyze the reforming of various plastics, such as polypropylene (PP), polystyrene (PS), and polyethylene terephthalate (PET), with CO₂ to produce CO and H₂ (Fig. 2b). With PP as reactant, the CO yield was slightly lower than with PE as reactant and more residual solid was left, which may be resulted from the recombination of radicals generated during the reaction at high temperature⁴¹. Furthermore, the residual solids amounts were higher for PS or PET than for PE or PP,

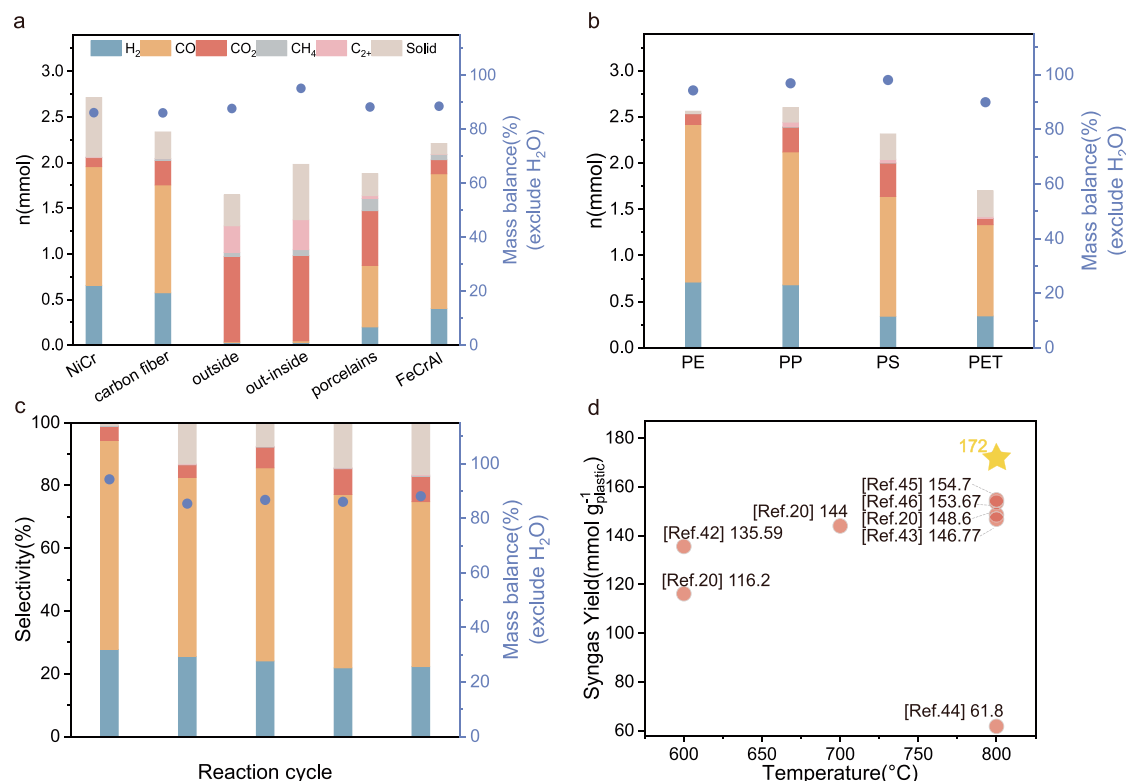


Fig. 2 | Catalytic performance under various conditions and the contrast with others system. a Product distribution of CO₂ reforming of PE using various heating components, Reaction conditions: PE = 14 mg, n(CO₂)/n(CH₂) = 1, T = 650 °C, 15 min; **b** CO₂ reforming of different plastics using electrified FeCrAl heating wire, Reaction conditions: PE = 14 mg, n(CO₂)/n(C of plastic) = 1, FeCrAl heating wire 6 Ω,

current 4 A, T = 800 °C, 15 min; **c** CO₂ reforming of PE using electrified FeCrAl heating wire, Reaction conditions: PE = 14 mg, n(CO₂)/n(CH₂) = 1, FeCrAl heating wire 6 Ω, current 4 A, T = 800 °C, 15 min; **d** the comparison of our result with ones from other reported catalytic system.

demonstrating the difficulty of destroying the benzene ring in PS or PET. As a result, the components that are difficult to be destroyed tends to be transformed into coke. Consequently, PE was selected as a candidate to carried out the exhaustive study. Furthermore, the FeCrAl heating wire can be reused at least five times without noticeably decreasing in the catalytic activity during CO₂ reforming of PE (Fig. 2c), showing excellent stability of the catalytic system. The slight decline in catalytic performance can be attributed to the carbon deposition and surface oxidation on the FeCrAl heating wire. Notably, compared to other reported systems requiring transition metal catalysts, the catalytic system based on the electrified heating wire exhibited competitive results (Fig. 2d)^{20,42–46}. Inspired by these results, various categories of real plastic product were selected as feedstocks, including pipette (PE), washing bottle (HDPE), mask (PE + PP), lunch box (PP), food container (PS), and bottle (PET) (Fig. 3a). The objective was to explore the potential of transforming these real plastic waste materials into CO and H₂ through the reforming process utilizing CO₂. Experimental results exhibited promising outcomes through the utilization of electrified FeCrAl heating wire, indicating the feasibility of converting mixed waste plastics (Fig. 3b). Furthermore, the scalability of the experiments was demonstrated by increasing the scale to 1 g of PE and the corresponding amount of CO₂. The large-scale reforming process (1 g PE and 3.3 g CO₂) was carried out in a large quartz tube (Fig. 3b; outer diameter = 60 mm, inner diameter = 50 mm, length = 1000 mm), resulting in a production of 2.84 g CO and 0.091 g H₂ within 30 min. This shows the potential for practical application in the field of heterogeneous catalysis. Actually, some carbon deposit (480 mg) on inner wall of the quartz tube can be observed. In addition, the productions of methane and other hydrocarbons were not negligible and small amount of CO₂ (110 mg) was also left (Supplementary Table 4). We conclude that the fast heat loss through the large-size quartz tube

results to the condensation of hydrocarbons. These condensed hydrocarbons cannot reform with CO₂ on the surface of heating wire and subsequently be converted into carbon deposit on the reactor wall. Therefore, in the practical large-scale experiment, some important factors, such as the pressure in the reactor, the distribution of the heating zone and the insulation technology for minimizing the heat loss, should all be considered.

The mechanism investigation

To understand the reaction mechanism, the kinetics of PE dehydrogenation, CO₂ reduction and CO₂ reforming of PE over electrified FeCrAl heating wire were investigated (Fig. 4). PE dehydrogenation can be easily carried out in argon atmosphere without CO₂. The yield of H₂ reached 28% within just 1 min of reaction time, while the yield of CH₄ was only 5%. As the electrification time progressed, the H₂ yield gradually increased, eventually achieving stoichiometric hydrogen production along with the formation of solid carbon. Notably, the methane yield showed a maximum throughout the reaction, suggesting that methane only served as an intermediate species during the PE dehydrogenation process. Additionally, the amount of residual solid initially decreased and then increased in the latter half of the reaction, further supporting the notion that PE was first cracked into gaseous products, and subsequently these gaseous hydrocarbons were dehydrogenated into hydrogen and solid carbon (Fig. 4a). The Fourier Transform infrared spectrometer (FTIR) spectra of solid at different reaction stage also indicate the destruction of the hydrocarbon structure in PE (Supplementary Fig. 4).

As a control experiment, we also investigated the reaction with CO₂ as the sole reactant over an electrified FeCrAl heating wire in the absence of PE. Surprisingly, a 66% yield of CO was detected and the conversion of CO₂ reached about 73% (Fig. 4b). Due to the lack of a

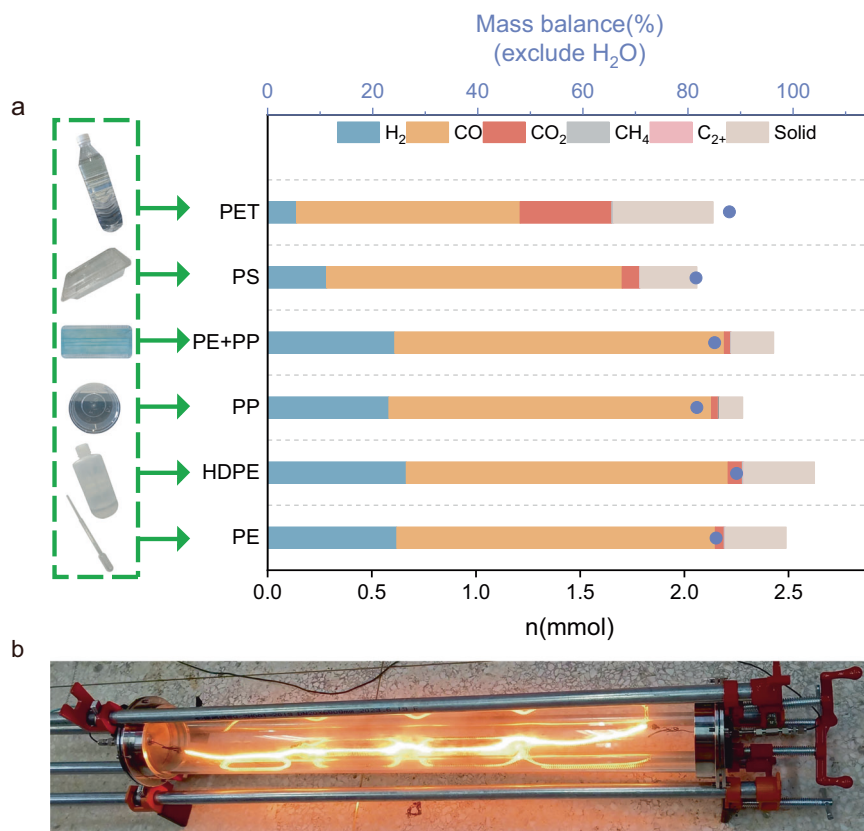


Fig. 3 | Catalytic performance for real plastic products and scale-up experiment. **a** CO₂ reforming of the real end-of-life plastics in the electrified system, reaction conditions: PE = 14 mg, $n(\text{CO}_2)/n(\text{C of plastic}) = 1$, FeCrAl heating wire 6 Ω ,

current 4 A, $T = 800^\circ\text{C}$, 15 min; **b** large-scale reactor for CO₂ reforming of plastics, reaction conditions: PE 1 g, CO₂ 3.3 g, FeCrAl heating wire 18 Ω , $T = 800^\circ\text{C}$, 30 min.

reducing agent in the system, we concluded that the metals present in the heating wire must be involved in the reaction and oxidized by CO₂. The weight of the heating wire did increase as the reaction progressed, which was consistent with the loss of oxygen in CO₂ during the reaction (see Supplementary Table 5). However, it is obvious that the CO₂ reduction over the electrified heating wire proved to be challenging. Even after a reaction time of 3 min, the yield of CO was less than 10% (Fig. 4b). In contrast, in the CO₂ reforming of PE under optimal reaction conditions, a 30% yield of CO could be achieved within just 1 min after the reaction (Fig. 4c). In comparison with PE dehydrogenation, the hydrogen yield decreased from 30% to 12%, and the measured amounts of hydrogen at different time intervals were lower in the standard reaction. Furthermore, the conversion rate of CO₂ was higher during CO₂ reforming of PE than during pure CO₂ reduction at the same reaction site. Therefore, we deduce that the hydrogen produced from the PE dehydrogenation was partially consumed to convert CO₂ to CO during the PE reforming with CO₂, suggesting that the reaction mechanism of CO₂ reforming of PE differs from that of simple PE dehydrogenation and CO₂ reduction.

To gain a deeper understanding of the reaction process, a FTIR was employed to monitor the gaseous products generated at different time intervals. The analysis revealed the presence of characteristic vibrations of CO (2100–2200 cm⁻¹) and hydrocarbon (2850–3200 cm⁻¹) after only 10 s of electrification (Fig. 4d). As the electrification time increased, the intensity of the CO characteristic vibrations became more pronounced, while the intensity of the hydrocarbon vibrations decreased. These observations provide further evidence that the initial decomposition of PE leads to the formation of small-molecule hydrocarbons, which subsequently react smoothly with CO₂ under optimal reaction conditions.

Furthermore, methane was employed as a representative small-molecule hydrocarbon, the reforming reaction over electrified FeCrAl heating wire was monitored by mass spectrometry in an argon gas flow. When methane was pulsed across the un electrified heating wire, there was no production of hydrogen or other products (Supplementary Fig. 5a). However, when methane was pulsed across the electrified heating wire, a peak in the signal of H₂ ($m/z = 2$) immediately appeared. At the same time, the intensity of the methane signal ($m/z = 15$) decreased compared to that over the non-electrified heating wire. This indicates that the pulsed methane was partially dehydrogenated into hydrogen and carbon over the electrified heating wire. Similarly, when CO₂ was pulsed over the non-electrified heating wire, peaks appeared intermittently in the MS signal of $m/z = 44$ and $m/z = 28$. This is because CO₂ ($m/z = 44$) can generate fragment ions of CO ($m/z = 28$) and O ($m/z = 16$) in MS (Supplementary Fig. 5b). It can be observed that the peak intensity of $m/z = 28$ increased significantly when CO₂ was pulsed into the electrified system, suggesting the generation of CO through the reduction of CO₂. These results demonstrate that the dehydrogenation of methane and the reduction of CO₂ can both occur individually on the electrified FeCrAl heating wire. However, by coupling these two individual reactions, carbon deposits from methane and oxygen from CO₂ on the surface of the FeCrAl heating wire can be effectively removed. The Raman spectra of heating wire at different electrified time show that the carbon species are deposited on it at initial stage and can be removed at the end of the reaction (Supplementary Fig. 6). Consequently, the catalytic CO₂ reforming of methane can be smoothly carried out on the electrified heating wire (right part of Fig. 4e).

To improve the understanding of the role of electrification on the FeCrAl heating wire, the system was modified by introducing only a length of FeCrAl heating wire and providing heat externally

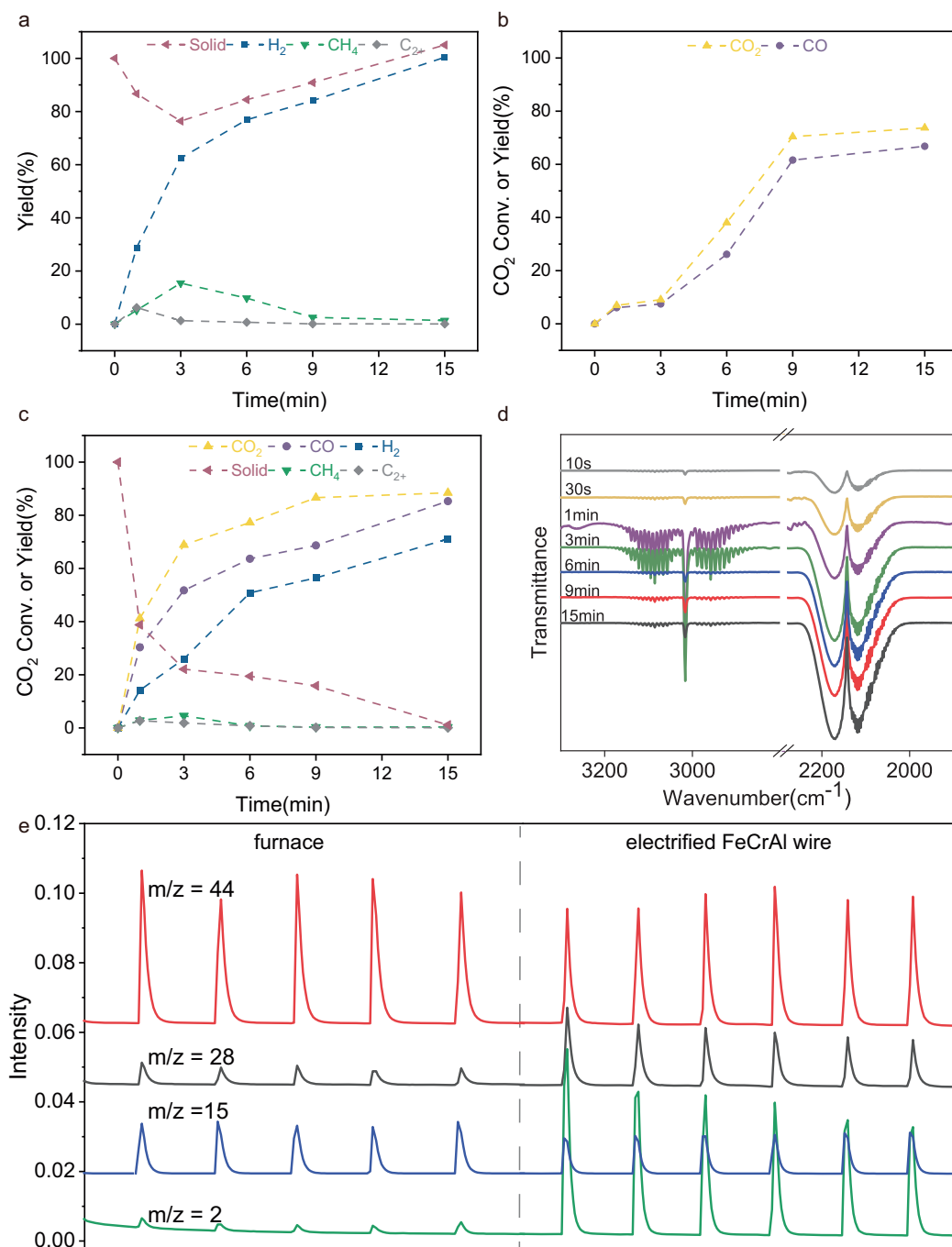


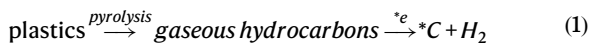
Fig. 4 | Catalysis kinetics parameters and the in-situ FTIR, MS analyses. **a** The kinetics of PE dehydrogenation on an electrified FeCrAl heating wire, reaction conditions: PE = 14 mg, Ar, FeCrAl heating wire 6 Ω , current 4 A, T = 800 $^{\circ}$ C, 15 min; **b** the kinetics of CO₂ reduction over an electrified FeCrAl heating wire; reaction conditions: n(CO₂) = 1 mmol, T = 800 $^{\circ}$ C, FeCrAl heating wire 6 Ω , 4 A, 15 min; **c** the kinetics of CO₂ reforming of PE on an electrified FeCrAl heating wire, reaction

conditions: PE = 14 mg, n(CO₂)/n(CH₄) = 1, FeCrAl heating wire 6 Ω , current 4 A, T = 800 $^{\circ}$ C, 15 min; **d** in-situ FTIR spectra of CO₂ reforming of PE on an electrified FeCrAl heating wire; **e** Mass spectrometry signals of CO₂ reforming of methane on a non-electrified FeCrAl heating wire heated using a furnace heating system, as well as on an electrified heating wire.

through a furnace. In this configuration, the FeCrAl heating wire remained unelectrified, but its temperature was the same as that of the electrified system. Upon injecting equimolar amounts of methane and CO₂ intermittently into the system, the mass spectrometry signals displayed peaks for m/z = 28 and m/z = 2. However, the intensities of these peaks were lower compared to the electrified system, as shown in Fig. 4e. This observation further

confirms that the FeCrAl heating wire has some catalytic activity towards the reaction, but electrification is crucial. Hence, we can conclude that the hot electrons on the heating wire initiate the dehydrogenation of the produced gaseous hydrocarbons from PE and the reduction of CO₂, as described by the following equations (Eqs. (1) and (2)). Some hydroxyls generate on the surface of the heating wire during the reforming process (Supplementary

Fig. 7)^{47,48}, which in turn facilitates dehydrogenation of PE through proton hopping and proton collision to gaseous hydrocarbons in the electric field^{49,50}. Subsequently, the carbon deposits then react with active oxygen species to produce additional CO molecules (Eq. (3)).



Life cycle assessment

Based on our experiments, a life cycle assessment (LCA) was conducted to evaluate the environmental impact of CO₂ reforming of plastic to produce syngas. The life cycle inventory based on the GREET 2022 was listed in the Supplementary Tables 6 and 7. This assessment was performed by analyzing the depletion of primary fossil energy (PFE) and the emission of greenhouse gases (GHG) using GREET 2022 software.

In our electrified system, the FeCrAl heating wire was functionalized as both a heating source and a catalytic component, eliminating the need for other catalysts. Consequently, the main contributor to GHG emissions and PFE depletion during the process is electricity consumption. This is because traditional LCA does not consider the construction of basic equipment and plants for large-scale chemical production. Figure 5a demonstrates that when using electricity from the Chinese electricity grids, the production of 1 kg of syngas with the electrified system results in GHG emissions of 341.29 kg and a PFE consumption of 6942 MJ (Fig. 5a). Because the energy consumption of the reforming system mainly focused on the electricity, the energy recovery efficiency is only 0.60% according to the corresponding calculations (Supplementary Tables 8 and 9). This procedure is just like to transform electric energy to chemical energy. To improve the sustainability and energy recovery efficiency of the electrified system for converting waste carbon sources (such as waste plastics and CO₂) into syngas, the electrified FeCrAl heating wire can be powered by a photovoltaic power system (PV) utilizing solar irradiation. As illustrated in Fig. 5b, the CO₂ reforming of PE can be smoothly carried out under natural solar irradiation in the solar-powered electrified system. This approach reduces PFE depletion and GHG emissions by 94.9% and 95.7%, respectively. More importantly, the energy recovery efficiency increases to

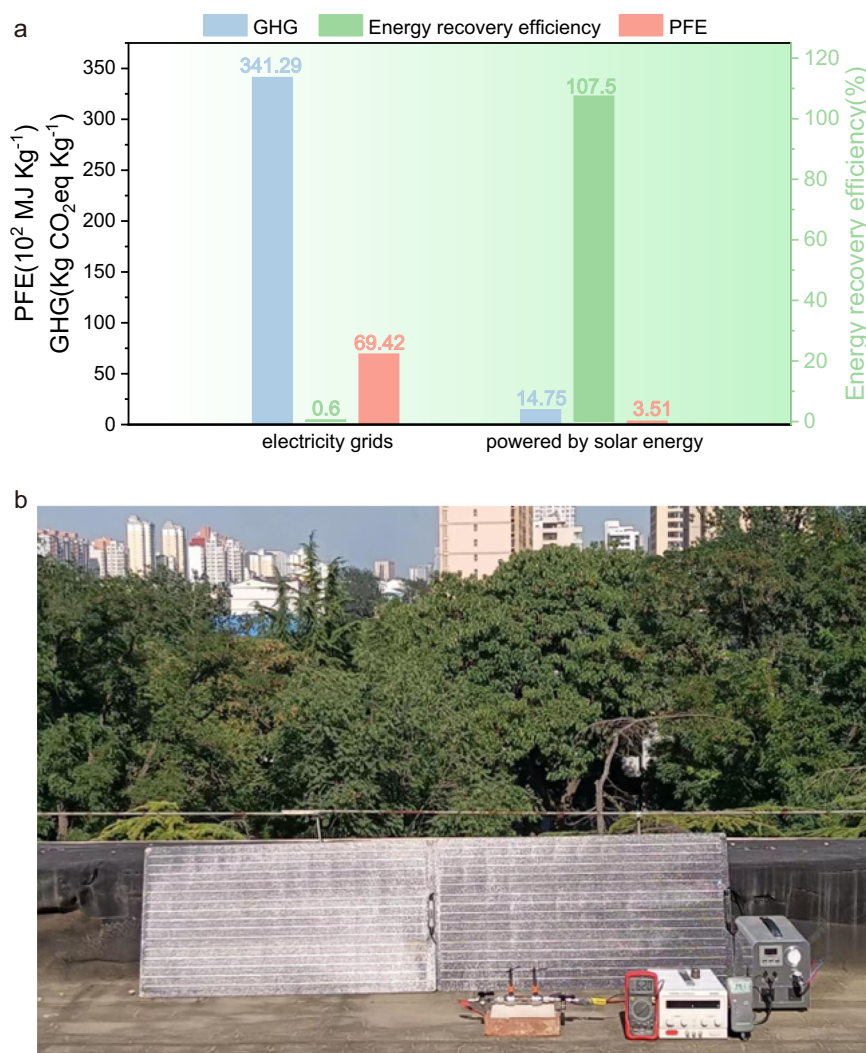


Fig. 5 | Life cycle assessment of the reforming system and a demo configuration using solar energy. **a** Effects of power supply methods on the life cycle PFE depletion, GHG emissions and energy recovery efficiency. **b** CO₂ reforming of PE

powered by photovoltaic power generation. reaction condition: 14 mg PE, 44 mg CO₂, FeCrAl heating wire 6 Ω, current 4 A, T = 800 °C, 15 min.

107.5%, showing a practical and potential strategy to store solar energy. Therefore, this environmentally friendly strategy for upcycling waste plastics and carbon dioxide is both sustainable and efficient, with the potential for application in a low-carbon future.

Discussion

The electrified FeCrAl heating wire serves as a crucial component for the CO₂ reforming of plastic into syngas. Not only does it provide high temperatures but it also acts as catalytically active sites and supports for hot electrons. Significantly, polyolefin plastics, such as PE and PP, can be effectively reformed with CO₂ to produce CO and H₂ with high yields and carbon balance. The plastics containing phenyl groups, such as PS and PET, can also be reformed with CO₂ to produce syngas, although relatively more residual carbon remained. However, prolonging the reaction time, the remained carbon will be less. Actually, the residual carbon derived from plastics with special nanostructure and without impurity may have other potential application. Indeed, Flash Joule Heating (FJH) technology has been used to convert plastics to one or two-dimension carbon nanomaterials in the presence of metal chloride as catalyst or carbon black as conductive additives^{51,52}. The achieved carbon nanotube must contain the metal nanoparticles and the conductive additive such as carbon black would impact the purity of the achieved graphene. Compared to the two FJH strategies, our reforming system with electrified heating wire as key component avoid the introduction of conductive additives or catalyst. In the absence of CO₂, PE can be dehydrogenated to carbon nanospheres (Supplementary Figs. 8 and 9) and hydrogen quantitatively. The carbon nanospheres mainly deposit on the heating wire and the inner wall of reactor, which make the separation from reactor easier than other reaction system.

Although the electrification for heating wire is the main energy consumption during the entire reaction according to the LCA result, it is an energy saving process because the internal heating strategy avoid the heat conduction and heat exchange in the traditional heating measures. The chemical energy of plastics is fully converted into the products syngas according to the calculated energy recovery efficiency. To facilitate the observation of the experimental phenomena, the main part of the reactor is designed as quartz tube without a heat insulator. By reducing the heat loss during the reaction, the energy consumption will be reduced. Moreover, the sustainability merit of this catalytic process can be further enhanced by using photovoltaic power under solar irradiation through a life-cycle assessment. Our approach not only offers a promising strategy for co-upcycling two waste carbon resources, but also paves the way for contributing to a sustainable circular economy.

However, some problems should be addressed if this kind of reforming reactor will be magnified and applied in the practical industry for the reforming of waste plastics and CO₂. Firstly, the reactor is a kind of batch reactor and the duration is crucial to comprehensively reform plastics with CO₂, which make it difficult to achieve the continuous feed of plastics and CO₂ to reactor. Even if the intermittent feeding is acceptable for the batch reactor, a feeding inlet should also be designed on the tube so that solid plastic can be fed around the heating wire. Secondly, in the large-scale reaction, considering the molar amount of CO₂ should be same with the molar amount of carbon in plastics in order to reform entirely, the volume of reactor should be large enough to accommodate the enough amount of CO₂. Consequently, the heating zone should be expanded to the whole reactor. In addition, insulation measures should be adopted to minimize the carbon deposit and ensure the reforming reaction entirely. More importantly, since the reforming reaction is a volume expansion process, safety for the experiment operator must be ensured. If a metal reactor is designed to improve the safety, the electric and thermal insulation must be taken into account to ensure

normal electrification and resistance to heat loss. The corresponding investigations are currently being carried out in our laboratory.

Method

Materials

All reagents were purchased from commercial suppliers and used as received. PE (1000 mesh, Shanghai Macklin Biochemical Technology Co., Ltd.), PP (MI:12 g/10 min, Shanghai Aladdin Biochemical Technology Co., Ltd.) and PET (300 mesh, Shanghai Branch, Du Pont China Holding Co., Ltd.) can be directly used. Standard Digital Multimeters (UNI-T, UT53) was used to measure temperature and resistance. FeCrAl wires involved in the experiment are made of the same material. A direct current (DC) power generator (MAISHENG, MP3030D) was used to supply power to the resistance wire. Outdoor solar power supply KUPA (KP220V, 600 W) provides electricity for PV system experiments. The partly reforming experiments (like heating rate comparison and MS experiment, Figs. 1d, 4e) were heated by an electrical furnace (Longkou Yuanbang Electric Furnace Manufacturing Co., Ltd.) which were separately temperature controlled and monitored.

CO₂ reforming of plastics

A length of spring-like iron-chromium-aluminum (FeCrAl) heating wire was cut from a long one with the diameter of 0.3 mm, and its resistance changes with its length. Fixing the heating wire on the metal terminals of a small porcelain boat with a dimension of 44 × 11 × 7 mm. After 14 mg of polyethylene (PE) was weighted into it, the porcelain boat was fixed into a quartz tube with an inner diameter of 19 mm and length of 100 mm, and two copper wires were connected with the two terminals of heating wire. Both ends of the quartz tube were sealed with rubber rings and metal flanges. On each metal flanges, one inlet equipped with a valve can connect with argon or CO₂ gas pipeline, and the copper wire connecting to heating wire came out from another inlet that was sealed with a rubber ring and a screw cap. The air in the system was purged out with a mixture gas (composed of 74% CO₂ and 26% Ar) and then filled with this mixture gas before reaction. The argon gas functions as internal gas for quantifying the gas products. Then a direct current (DC) power generator (MAISHENG, MP3030D) was used to supply power to the resistance wire. The current and voltage were adjusted according to the experimental demand. The temperature in the reactor was detected with a thermal couple inserted into the system and the temperature distribution of the reaction system was recorded by an infrared thermal imager (UTi-260B, Uni-Trend Technology Co., Ltd.). The gas products were analyzed and quantified by a gas chromatography (Agilent 7820 A) equipped with thermal conductivity detector (TCD) and flame ionization detector (FID). A Haysep Q column was connected to TCD to analyze CO, H₂ and Ar, and a HP-PLOT Al₂O₃ column connecting to FID was used to analyze methane and other hydrocarbons. The inlet temperature was set at 200 °C. The carrier gas was He with flow rate of 3 mL min⁻¹. Because the carbon residual mainly deposits on the boat, resistance wire and quartz tube, the mass of solid was determined by weighing the total mass of the three parts before and after reaction. In detail, the weight of solid product was calculated by the difference between after reaction and before reaction (Supplementary Table 1).

The carbon balance and mass balance of each reaction:

$$\text{carbon balance} = \frac{n_{\text{CO}} + n_{\text{CO}_2}(\text{on GC}) + n_{\text{C}_2\text{H}_6} + 2n_{\text{C}_2\text{H}_4} + 3\text{C}_3\text{H}_8 + \frac{m_{\text{solid}}}{12}}{\frac{m_{\text{PE}}}{14} + n_{\text{CO}_2}(\text{original})} \times 100\% \quad (4)$$

$$\text{mass balance} = \frac{2n_{\text{H}_2} + 28n_{\text{CO}} + 44n_{\text{CO}_2}(\text{on GC}) + 16n_{\text{C}_2\text{H}_6} + 30n_{\text{C}_2\text{H}_4} + 28n_{\text{C}_2\text{H}_4} + 44\text{C}_3\text{H}_8 + m_{\text{solid}}}{m_{\text{PE}} + m_{\text{CO}_2}(\text{original})} \times 100\% \quad (5)$$

For other plastics, such as polypropene (PP), polystyrene (PS), polyethylene terephthalate (PET), the loading mass was determined by maintaining equal moles of carbon in plastics and CO₂.

In-situ Fourier Transform Infrared spectrum (FTIR)

A home-made gas cell having two parallel zinc selenide windows and a Fourier transform infrared spectrometer (Thermo NICOLET IS-10) were used to record the spectrum. At different reaction stage, the gas product was sampled and injected into the gas cell to collect the FTIR spectrum.

In-situ pulsed Mass spectrum (MS)

With methane as representative hydrocarbon, the pulsed dry reforming of methane was monitored by online mass spectrometry (Hiden, HPR-40). The argon gas with a flow rate of 10 mL/min was used as employed as a carrier gas. Methane, CO₂ or the mixture of CO₂ and CH₄ was pulsed injected into the reactor through a six-way valve equipped a quantitative ring (1.8 mL) after the baseline was flat. The m/z values of 44, 28, 15, 2 were all monitored by the online MS.

Life cycle assessment

We used the GREET 2022 software to perform Life Cycle Assessment (LCA) calculations such as greenhouse gas (GHG) emission and primary fossil energy (PFE) depletion, evaluating environment impacts within different system. Parameter and values are presented for calculation model and PV system in Supplementary Tables 6 and 7.

Energy recovery efficiency

To estimate the reforming system, we defined energy recovery efficiency as following. The main reforming products of our work were gases. Herein, the energy recovery efficiency was calculated according to this:

$$\text{energy recovery efficiency} = \frac{\text{output energy}}{\text{PE chemical energy} + \text{electricity energy}} \times 100\% \quad (6)$$

The detailed calculated information was shown in Supplementary Tables 8 and 9.

Data availability

The data that support the figures within this paper and another finding of this study are available from the corresponding author upon request. Source data are provided as a Source Data file. Source data are provided with this paper.

References

1. Plastic upcycling. *Nat. Catal.* **2**, 945–946 <https://doi.org/10.1038/s41929-019-0391-7> (2019).
2. Coates, G. W. & Getzler, Y. D. Y. L. Chemical recycling to monomer for an ideal, circular polymer economy. *Nat. Rev. Mater.* **5**, 501–516 (2020).
3. Geyer, R., Jambeck, J. R. & Law, K. L. Production, use, and fate of all plastics ever made. *Sci. Adv.* **3**, e1700782 (2017).
4. Tournier, V. et al. An engineered PET depolymerase to break down and recycle plastic bottles. *Nature* **580**, 216–219 (2020).
5. Montes, D. et al. Combustion behaviour of plastic waste—a case study of PP, HDPE, PET, and mixed PES-EL. *J. Clean Prod.* **402**, <https://doi.org/10.1016/j.jclepro.2023.136850> (2023).
6. Liu, Z., Deng, Z., Davis, S. & Ciais, P. Monitoring global carbon emissions in 2022. *Nat. Rev. Earth Environ.* **4**, 205–206 (2023).
7. Li, H. et al. Hydroformylation of pyrolysis oils to aldehydes and alcohols from polyolefin waste. *Science* **381**, 660–666 (2023).
8. Torelli, D. A. et al. Nickel–gallium–catalyzed electrochemical reduction of CO₂ to highly reduced products at low overpotentials. *ACS Catal.* **6**, 2100–2104 (2016).
9. Zhang, M.-Q. et al. Catalytic strategies for upvaluing plastic wastes. *Chem* **8**, 2912–2923 (2022).
10. Lee, K., Jing, Y., Wang, Y. & Yan, N. A unified view on catalytic conversion of biomass and waste plastics. *Nat. Rev. Chem.* **6**, 635–652 (2022).
11. Zhao, Y. et al. Solar- versus thermal-driven catalysis for energy conversion. *Joule* **3**, 920–937 (2019).
12. Zhang, X. et al. Carbonate hydrogenated to formate in the aqueous phase over Nickel/TiO₂ catalysts. *Angew. Chem. Int. Ed.* **62**, e202307061 (2023).
13. Liu, Y. et al. Intensifying hydrogen heterocrossing via regulating the ZnO overlayer for enhanced fatty acid ester hydrogenation. *ACS Catal.* 16126–16135 <https://doi.org/10.1021/acscatal.3c05013> (2023).
14. Yuan, S. et al. Highly active sunlight-driven CO₂ methanation catalyst: design of the interfacial structure. *Fuel* **335**, <https://doi.org/10.1016/j.fuel.2022.126855> (2023).
15. Bu, X. et al. Reaction mechanism insights into CH₄ catalytic oxidation on Pt13 cluster: a DFT study. *Mol. Catal.* **515**, <https://doi.org/10.1016/j.mcat.2021.111891> (2021).
16. Chen, H., Xu, X., Fang, C., Li, B. & Nie, M. Differences in the temperature dependence of wetland CO₂ and CH₄ emissions vary with water table depth. *Nat. Clim. Chang.* **11**, 766–771 (2021).
17. Wang, S., Lu, G. Q. & Millar, G. J. Carbon dioxide reforming of methane to produce synthesis gas over metal-supported catalysts: state-of-the-art. *Energy Fuels* **10**, 896–904 (1996).
18. Yuan, S. et al. CO₂ methanation boosted by support-size-dependent strong metal-support interaction and B–O–Ti component. *Green Energy Environ.* <https://doi.org/10.1016/j.gee.2022.05.010> (2022).
19. Jung, S. et al. CO₂-mediated thermal treatment of disposable plastic food containers. *Chem. Eng. J.* **451**, <https://doi.org/10.1016/j.cej.2022.138603> (2023).
20. Saad, J. M. & Williams, P. T. Pyrolysis-catalytic dry (CO₂) reforming of waste plastics for syngas production: influence of process parameters. *Fuel* **193**, 7–14 (2017).
21. Luo, J. et al. Leveraging CO₂ to directionally control the H₂/CO ratio in continuous microwave pyrolysis/gasification of waste plastics: Quantitative analysis of CO₂ and density functional theory calculations of regulation mechanism. *Chem. Eng. J.* **435**, <https://doi.org/10.1016/j.cej.2022.134794> (2022).
22. Zhang, F. et al. Polyethylene upcycling to long-chain alkyaromatics by tandem hydrogenolysis/aromatization. *Science* **370**, 437–441 (2020).
23. St. John, P. C., Guan, Y., Kim, Y., Kim, S. & Paton, R. S. Prediction of organic homolytic bond dissociation enthalpies at near chemical accuracy with sub-second computational cost. *Nat. Commun.* **11**, 2328 (2020).
24. Zolghadr, A. et al. On the method of pulse-heated analysis of solid reactions (PHASR) for polyolefin pyrolysis. *ChemSusChem* **14**, 4214–4227 (2020).
25. Borisov, V. A. et al. Carbon deposits on a resistive FeCrAl catalyst for the suboxidative pyrolysis of methane. *Kinet. Catal.* **55**, 319–326 (2014).
26. Ambrosetti, M. A perspective on power-to-heat in catalytic processes for decarbonization. *Chem. Eng. Process.* **182**, 109187 (2022).
27. Zheng, L., Ambrosetti, M. & Tronconi, E. Joule-heated catalytic reactors toward decarbonization and process intensification: a review. *ACS Eng. Au* **4**, 4–21 (2024).
28. Dong, Q. et al. Depolymerization of plastics by means of electrified spatiotemporal heating. *Nature* **616**, 488–494 (2023).

29. Wang, W., Zhao, S., Tang, X., Chen, C. & Yi, H. Electrothermal catalysis for heterogeneous reaction: mechanisms and design strategies. *Chem. Eng. J.* **455**, <https://doi.org/10.1016/j.cej.2022.140272> (2023).
30. Kim, Y. T., Lee, J.-J. & Lee, J. Electricity-driven reactors that promote thermochemical catalytic reactions via joule and induction heating. *Chem. Eng. J.* **470**, <https://doi.org/10.1016/j.cej.2023.144333> (2023).
31. Nagireddi, S., Agarwal, J. R. & Vedapuri, D. Carbon dioxide capture, utilization, and sequestration: current status, challenges, and future prospects for global decarbonization. *ACS Eng. Au* **4**, 22–48 (2024).
32. Pauletto, G. et al. FeCrAl as a catalyst support. *Chem. Rev.* **120**, 7516–7550 (2020).
33. Kondofersky, I. et al. Nanostructured ternary FeCrAl oxide photocathodes for water photoelectrolysis. *J. Am. Chem. Soc.* **138**, 1860–1867 (2016).
34. Kaltner, W., Veprek-Heijman, M., Jentys, A. & Lercher, J. A. Effect of chromium migration from metallic supports on the activity of diesel exhaust catalysts. *Appl. Catal. B Environ.* **89**, 123–127 (2009).
35. Setiawan, A., Kennedy, E. M. & Stockenhuber, M. Development of combustion technology for methane emitted from coal-mine ventilation air systems. *Energy Technol.* **5**, 521–538 (2017).
36. Frost, L., Elangovan, E. & Hartvigsen, J. Production of synthetic fuels by high-temperature co-electrolysis of carbon dioxide and steam with Fischer-Tropsch synthesis. *Can. J. Chem. Eng.* **94**, 636–641 (2016).
37. Merino, D., Sanz, O. & Montes, M. Effect of the thermal conductivity and catalyst layer thickness on the Fischer-Tropsch synthesis selectivity using structured catalysts. *Chem. Eng. J.* **327**, 1033–1042 (2017).
38. He, L. et al. Microstructure, oxidation and corrosion properties of FeCrAl coatings with low Al content prepared by magnetron sputtering for accident tolerant fuel cladding. *J. Nucl. Mater.* **551**, 152966 (2021).
39. Studer, A. & Curran, D. P. The electron is a catalyst. *Nat. Chem.* **6**, 765–773 (2014).
40. Chen, H. et al. Electron-catalyzed dehydrogenation in a single-molecule junction. *J. Am. Chem. Soc.* **143**, 8476–8487 (2021).
41. Ahmad, I. et al. Pyrolysis study of polypropylene and polyethylene into premium oil products. *Int. J. Green. Energy* **12**, 663–671 (2015).
42. Zou, J., Zhao, L., Hu, Q., Yao, D. & Yang, H. Pyrolysis and catalytic reforming of disposable plastic waste for syngas production with adjustable H₂/CO ratio. *Appl. Energy* **362**, <https://doi.org/10.1016/j.apenergy.2024.122844> (2024).
43. Saad, J. M. & Williams, P. T. Manipulating the H₂/CO ratio from dry reforming of simulated mixed waste plastics by the addition of steam. *Fuel Process. Technol.* **156**, 331–338 (2017).
44. Zhang, X. et al. CO₂-mediated catalytic upcycling of plastic waste for H₂-rich syngas and carbon nanomaterials. *J. Hazard. Mater.* **460**, <https://doi.org/10.1016/j.jhazmat.2023.132500> (2023).
45. Saad, J. M. & Williams, P. T. Pyrolysis-catalytic-dry reforming of waste plastics and mixed waste plastics for syngas production. *Energy Fuels* **30**, 3198–3204 (2016).
46. Saad, J. M. & Williams, P. T. Catalytic dry reforming of waste plastics from different waste treatment plants for production of synthesis gases. *Waste Manag.* **58**, 214–220 (2016).
47. Biedrzycka, A., Skwarek, E. & Hanna, U. M. Hydroxyapatite with magnetic core: synthesis methods, properties, adsorption and medical applications. *Adv. Colloid Interface Sci.* **291**, 102401 (2021).
48. Singh, A. K., Talat, M., Singh, D. P. & Srivastava, O. N. Biosynthesis of gold and silver nanoparticles by natural precursor clove and their functionalization with amine group. *J. Nanopart. Res.* **12**, 1667–1675 (2010).
49. Zhang, J., Nakaya, Y., Shimizu, K. I. & Furukawa, S. Surface engineering of titania boosts electroassisted propane dehydrogenation at low temperature. *Angew. Chem. Int. Ed.* **62**, e202300744 (2023).
50. Yabe, T. et al. Role of electric field and surface protonics on low-temperature catalytic dry reforming of methane. *ACS Sustain. Chem. Eng.* **7**, 5690–5697 (2019).
51. Wyss, K. M. et al. Upcycling of waste plastic into hybrid carbon nanomaterials. *Adv. Mater.* **35**, e2209621 (2023).
52. Wyss, K. M. et al. Synthesis of clean hydrogen gas from waste plastic at zero net cost. *Adv. Mater.* **35**, <https://doi.org/10.1002/adma.202306763> (2023).

Acknowledgements

The authors acknowledge the fund support of the National Natural Science Foundation of China (22378094, 22232001), Natural Science Foundation of Hebei Province (B2023201108). D.M. acknowledges support from the Tencent Foundation through the XPLOER PRIZE and the New Cornerstone Science Foundation. We thank Dr. Meng Wang for proofreading.

Author contributions

Q.M. carried the experiments out, Y.G. conceived the experiment and wrote the paper, and together with B.S. and D.M.; J.D. and H.Z. carried out the data analysis. All authors contribute to the discussion and revision of the paper.

Competing interests

The authors declare no competing interests.

Additional information

Supplementary information The online version contains supplementary material available at <https://doi.org/10.1038/s41467-024-52515-y>.

Correspondence and requests for materials should be addressed to Yongjun Gao or Ding Ma.

Peer review information *Nature Communications* thanks the anonymous reviewers for their contribution to the peer review of this work. A peer review file is available.

Reprints and permissions information is available at <http://www.nature.com/reprints>

Publisher's note Springer Nature remains neutral with regard to jurisdictional claims in published maps and institutional affiliations.

Open Access This article is licensed under a Creative Commons Attribution-NonCommercial-NoDerivatives 4.0 International License, which permits any non-commercial use, sharing, distribution and reproduction in any medium or format, as long as you give appropriate credit to the original author(s) and the source, provide a link to the Creative Commons licence, and indicate if you modified the licensed material. You do not have permission under this licence to share adapted material derived from this article or parts of it. The images or other third party material in this article are included in the article's Creative Commons licence, unless indicated otherwise in a credit line to the material. If material is not included in the article's Creative Commons licence and your intended use is not permitted by statutory regulation or exceeds the permitted use, you will need to obtain permission directly from the copyright holder. To view a copy of this licence, visit <http://creativecommons.org/licenses/by-nc-nd/4.0/>.

© The Author(s) 2024